

See discussions, stats, and author profiles for this publication at: <https://www.researchgate.net/publication/327845270>

Data-driven proton exchange membrane fuel cell degradation predication through deep learning method

Article in Applied Energy · December 2018

DOI: 10.1016/j.apenergy.2018.09.111

CITATIONS
16

READS
1,032

6 authors, including:



Rui Ma
Université de Technologie de Belfort-Montbéliard

40 PUBLICATIONS 100 CITATIONS

[SEE PROFILE](#)



Tao Yang
Université de Technologie de Belfort-Montbéliard

9 PUBLICATIONS 27 CITATIONS

[SEE PROFILE](#)



Elena Breaz
Universitatea Tehnica Cluj-Napoca

41 PUBLICATIONS 310 CITATIONS

[SEE PROFILE](#)



Zhongliang Li
Aix-Marseille Université

33 PUBLICATIONS 205 CITATIONS

[SEE PROFILE](#)

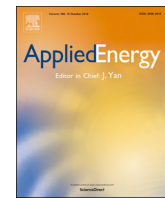
Some of the authors of this publication are also working on these related projects:



Fuel Cells project [View project](#)



Fabrication of large size protonic ceramic cell: high performanc and reliability [View project](#)



Data-driven proton exchange membrane fuel cell degradation predication through deep learning method



Rui Ma^{a,b,f,*}, Tao Yang^c, Elena Breaz^{a,b}, Zhongliang Li^d, Pascal Briois^e, Fei Gao^{a,b}

^a FEMTO-ST Institute, Univ. Bourgogne Franche-Comté, UTBM, CNRS, F-90010 Belfort Cedex, France

^b FCLAB, Univ. Bourgogne Franche-Comté, UTBM, CNRS, Rue Thierry Mieg, F-90010 Belfort Cedex, France

^c Le2i (UMR CNRS 6306), FRE2005, Arts et Métiers, Univ. Bourgogne Franche-Comté, UTBM, F-90010 Belfort Cedex, France

^d LIS Laboratory (UMR CNRS 7020), Aix-Marseille University, 13397 Marseille, France

^e FEMTO-ST (UMR CNRS 6174), MN2S Department, Univ. Bourgogne Franche-Comté, UTBM, 25200 Montbéliard, France

^f School of Automation, Northwestern Polytechnical University, 710072 Xi'an, China

HIGHLIGHTS

- Deep learning method is used to predict fuel cell degradation.
- G-LSTM cell based RNN is deployed for the prognostic.
- Aging experimental tests with different fuel cells are conducted.
- The G-LSTM can make predictions within the same framework.
- The proposed prognostic model can be applied to online diagnosis.

ARTICLE INFO

Keywords:

Fuel cell
Prognostics
Degradation model
Long short-term memory
Deep machine learning

ABOUT THE ARTICLE

Proton exchange membrane fuel cells (PEMFCs) is one of the principal candidates to take part of the worldwide future clean and renewable energy solution. However, fuel cells are vulnerable to the impurities of hydrogen and operating conditions, which could cause the degradation of output performance over time during operation. Thus, the prediction of the performance degradation draws attention lately and is critical for the reliability of the fuel cell system. In this work, we propose an innovative fuel cell degradation prediction method using Grid Long Short-Term Memory (G-LSTM) recurrent neural network (RNN). Long short-term memory cell can effectively avoid the gradient exploding and vanishing problem compared with conventional neural network architecture, which makes it suitable for the prediction problem for long period. By paralleling and combining the cells, Grid long short-term memory cell architecture can further optimize the prediction accuracy of the fuel cell performance degradation. The proposed prediction model is experimentally validated by three different types of PEMFC: 1.2 kW Ballard Nexa fuel cells, 1 kW Proton Motor fuel cells and 25 kW Proton Motor fuel cells. The results indicate that the proposed Grid long short-term memory network can predict the fuel cell degradation in a precise way. The proposed deep learning approach can be efficiently applied to predict the lifetime of fuel cell in transportation applications.

1. Introduction

Fuel cell technology is considered one of the most attractive power sources for future transportation system due to the concerns for environment preservation and fossil fuels depletion [1]. Among different fuel cells types, proton exchange membrane fuel cell (PEMFC) is considered the most suitable one for automotive applications due to its low operating temperature, higher power density and short start time.

Thanks to the advancement in material engineering, the PEMFC can now satisfy the power demand and operating requirements of vehicular applications. However, the fuel cell lifetime should still be increased in order to meet the requirements of transportation applications.

The degradation performance of PEMFCs is strongly influenced by the operating conditions [2]. Durability is a main concern to successful deploy the fuel cell system on the market [3]. Thus, in order to control efficiently the fuel cell system and maximize the fuel cell lifetime, the

* Corresponding author at: School of Automation, Northwestern Polytechnical University, 710072 Xi'an, China.
E-mail address: rui.ma@utbm.fr (R. Ma).

degradation phenomena should be understood in a clear way and be able to be predicted by a precisely degradation model.

The fuel cell degradation model can usually be classified into two categories: model based and data based. Most of the researches in literature conduct the degradation prediction through building semi-empirical models [4–11]. The fuel cell degradation in both electrical and mechanical domains are analyzed to predict the voltage drop as the operating time increased. The electrodes and electrolyte degradations are also discussed in order to develop the prediction models. One of the advantages of the model-based methods is that they do not require a large amount of experimental data. However, all these proposed semi-empirical models still depend on experimental measurements and must be previously adapted for different types of fuel cells to be able to predict the performance degradation.

In order to improve the adaptability and the accuracy of the degradation model, data-driven degradation predictions and diagnostic methods are adopted to fuel cell related applications recently. In [12] the authors proposed a hybrid data-driven method combined with conventional model-based approach for PEMFC prognostics. Procedures for data selection and processing are proposed, whereas the proposed method still suffers from computational issues, which is not suitable for online diagnostic problem. Another work dedicating PEMFC prognostics has been proposed by Javed et al. in [13]. The presented model used a constraint based summation wavelet extreme learning machine (SW-ELM) to improve the robustness and the applicability of long-term prognostics of PEMFC for online applications. The developed algorithm is able to predict PEMFC lifetime under dynamic load conditions as well. Similar works have been proposed by Ibrahim et al. in [14]. The authors deployed a wavelet-based approach for online fuel cell remaining useful lifetime prediction. A prognostics method based on adaptive neuro-fuzzy inference systems is proposed to make long-term prognostics for PEMFCs by using the filtered data in [15]. However, these works are all focused on the long-term prognostic of the fuel cell. It is well known that, the short-term prognostics is also very important for the fuel cell lifetime and energy management systems. By applying the Kalman Filter into industrial applications, particle filter has been successfully deployed for the prognostics of the fuel cell in [16–18]. Mathieu et al. [16] proposed a prognostic method for the fuel cell by an observer based on an Extended Kalman Filter. The state of health and the dynamic of the degradations is estimated. Although the proposed methods are effective for the prognostics, analytical degradation models still need to be built in prior. A holistic solution towards prognostics of industrial PEMFC is proposed in [17]. Although it involves an efficient multi-energetic model suited for diagnostics and prognostics, the prediction by using this model has not yet been fully developed. Similar work in [18] used particle filtering framework. However, the model cannot make degradation predication. Wu et al. [19,20] proposed a fuel cell prognostic method by using the relevance vector machine (RVM). The authors have modified and improved the basic RVM algorithm and achieved higher prediction accuracy for both short and long-term prediction. However, the prediction RVM model needs to be re-trained from scratch once the fuel cell operating conditions change. Research work in [21] used cyclic voltammetry and linear sweep voltammetry to estimate the internal statement of the fuel cell stack. Although it is a commonly used diagnostic approach, the prediction of the degradation cannot be done online in practical applications. Li et al. [22,23] proposed an effective long-term prognostics algorithm based on mode space learning. The prognosis-oriented features are firstly fitted by a series signal segments, and then extracted from the model parameters. The remaining useful life estimation of PEMFCs under certain current profiles can be obtained, whereas the short-term performance is not discussed. Onanena et al. contributed to the prognostic on fuel cell in [24]. Both the static and dynamic information extracted from the stack, which include polarization curve records and electrochemical impedance spectroscopy (EIS) measurement, can be used for the proposed pattern-recognition-based diagnosis approach to

estimate the remaining useful life of PEMFCs. EIS method is also deployed in [25] for the degradation prognostic of the fuel cell. Since additional efforts of EIS measurement and calculation are required, the proposed method cannot be directly used for online diagnostic control.

As can be seen from the previous mentioned literature, most of the prognostic methods use the fuel cell output voltage value to monitor the performance degradation. Thus, we can simply regard the degradation prediction as a time series problem, and model it using machine-learning methods. Among different kinds of neural networks, recurrent neural network (RNN) is suitable for the series data processing, which can be applied to the fuel cell degradation prediction problem. Liu et al. [26] proposed a combined wavelet analysis and the group method of data handing (W-GMDH). Although the model accuracy can reach the degradation prediction requirement, the proposed method is not capable to forecast the degradation in a future time. Suk et al. [27] proposed an accelerated degradation test (ADT) approach to reduce the fuel cell degradation testing time. Although the degradation trend can be obtained, the ADT may bring errors since the real degradation trend cannot be fully simulated. Morando et al. [28,29] deployed a PEMFC ageing forecasting algorithm based on the echo state network. The network must be trained with filtered data, and many parameters need to be configured for fuel cell voltage ageing forecasting, which makes the proposed method difficult to apply. However, the results obtained with a Mean Average Percentage Error (MAPE) of less than 5% prove the effectiveness of RNN based predicting approach.

The Long Short-Term Memory network (LSTM) is a type of RNN that achieves state-of-the-art results on challenging prediction problems. Deep learning methods like LSTM can be used to predict time series problem for both short and long periods. Compared with traditional RNN, LSTM is capable to avoid gradient exploding and gradient vanishing problem, which can make the short-term memory last for a long period of time [30]. Fuel cell aging under thousands hours operating makes LSTM suitable as a degradation prediction approach. The simple architecture also enables LSTM to be easily applied to online diagnostic control, which can help to design and verify the fuel cell system control methods [31]. In this paper, an innovative deep learning data-driven model for PEMFC degradation prediction is proposed based on LSTM network, which has never been discussed in the literature. Moreover, based on the conventional LSTM network, the paper proposes a Grid LSTM (G-LSTM) architecture to further improve the prediction accuracy. The proposed model is then verified by experimental aging test results of three different types of PEM fuel cells under eight different operating conditions. The main contributions of this paper can be summarized as follows:

1. Fuel cell degradation experiments are conducted with 8 different fuel cells under various operating conditions. The operating time ranges from hundreds of hours to ten thousand hours. All experimental aging data is recorded to evaluate the fuel cell operating performance.
2. Based on the conventional Recurrent Neural Network (RNN), the long short-term memory (LSTM) cell is added in order to avoid gradient vanishing and exploding. Such a deep learning method is then originally applied to the degradation prediction of the fuel cell.
3. Based on the basic LSTM cell, a Grid LSTM architecture is proposed and implemented to predict the fuel cell degradation. The corresponding training algorithm is designed to predict the degradations of different fuel cells under the same framework. The performance of the proposed deep learning G-LSTM RNN is verified by the experimentally measured degradation data.

The paper is organized as follows: Section 2 presents the fuel cell configurations, and their aging experimental test results under varies operating conditions. The deep learning approach by G-LSTM network is developed and analyzed in Section 3. In Section 4, the model prediction results are compared with the previous experimental measured

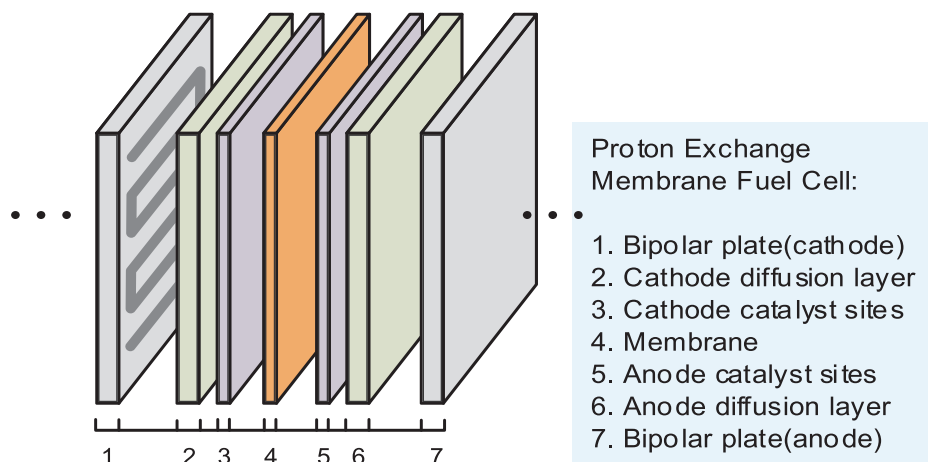


Fig. 1. Fuel cell elementary structure in the stack.

results along with the discussions. At last, conclusions are given in [Section 5](#).

2. Fuel cell aging experimental implementation

To understand better the fuel cell operation principles, a brief introduction of PEMFC is given first in this section. Then, the aging experimental test conditions and results are described for three different types of PEMFC including NEXA Ballard 1.2 kW fuel cells and Proton Motor 200 (PM200) 1 kW and 25 kW fuel cells.

2.1. Proton exchange membrane fuel cells

2.1.1. Fuel cell elementary structure

The single cell elementary structure of PEMFC is shown in [Fig. 1](#). During the fuel cell operation, the oxygen will flow into the cathode electrode whereas the hydrogen will flow into the anode electrode.

The typical PEMFC power range is from a few milliwatts to a few hundred kilowatts. In order to provide electricity, the oxydo-reduction electrochemical reactions will occur in the fuel cell stack when the oxygen and hydrogen diffuse to the triple phase boundary (TPB) as:



The fuel cell stack is usually formed by individual cells, and the output voltage can be obtained by the summary of the series fuel cells voltage. Along with the increasing of operating time, the membrane and the electrode of fuel cell will age and thus influence output performance.

2.1.2. Fuel cell degradation phenomena

During fuel cell operation, all its components can degrade or fail to function, thus causing the PEMFC degradation or failure [\[32\]](#). The degradation mechanisms of fuel cell layers are usually influenced by each other, and most of the degradations take place in gas diffusion layer (GDL), catalyst layer and polymer membrane [\[3\]](#). Generally, the GDL is made of carbon paper or cloth and the major degradation phenomenon of GDL is carbon corrosion. In most cases, a serious carbon corrosion is usually caused by of high humidity and/or frequent potential (load) cycling of the PEMFC [\[33,34\]](#). Platinum (catalyst) dissolution or reorganization (sintering) in the catalyst layer are also commonly considered as critical factors influencing long-term performance of PEMFC. The platinum particles are attached on the surface of carbon support in electrodes, so it is vulnerable when carbon structure starts to degrade. Besides, the platinum particles sintering can be commonly observed under load cycling and/or operating conditions

such as high humidity or high temperature [\[35\]](#). For the polymer membrane, it is believed that the chemical attacks caused by hydroxyl (OH^-) and hydroperoxyl (OOH^-) radicals initiate the membrane degradation. These radicals are stemmed from hydrogen peroxide (H_2O_2) which is formed due to either contamination of fuels or gas crossover. The chemical attack along with the transient operating conditions results in polymer structure degradation and the modification of membrane properties [\[36\]](#).

In addition, the membrane electrode assembly (MEA) durability is highly influenced by the start – stop cycles [\[2\]](#). If the fuel cell is stopped for long time, the hydrogen can cross over from the anode to the cathode, and the anode channels will be filled with air. When this happens, fuel cell start-up will create a transient condition in which fuel exists at the inlet but the outlet is still fuel-starved at the anode side. This localized fuel starvation can induce the local potential at the cathode to be higher than 1.8 V, which will cause important degradations on MEA [\[37\]](#).

Since the degradants happen at the electrodes and interfaces, the stack performance starts to decay and thus affects the system's efficiency [\[38\]](#). The major degradation mechanisms and their causes are summarized in [Table 1](#).

2.2. Aging experiments for fuel cell

2.2.1. Ballard NEXA fuel cell

The aging experimental tests of 1.2 kW Ballard NEXA fuel cell stack, which contains 47 cells, are conducted first. The fuel cells are operated under steady-state conditions of 12 A/30 °C, 30 A/35 °C, 36 A/40 °C and 44 A/40 °C, respectively. [Fig. 2](#) shows the experimental fuel cell test bench. The stack temperature is measured by the infrared camera, and the voltage is measured by the plug-in sensors.

In these aging experiments, the fuel cell load is set to be constant. The individual cell voltages are measured continually for 400 h, and the temperature variations of the fuel cell is monitored. All the measured data are stored in the supervising computer. [Table 2](#) shows the detailed fuel cell operating conditions.

Table 1
Causes & effects of PEMFC degradation.

	Carbon corrosion	Platinum loss	Membrane degradation
Elec. potential	Cycling potential	Cycling potential	Potential cycling
Humidity	High	High	Cycling humidity
Load	Cycling load	Low/cycling load	Cycling load
Temperature	High	High	High

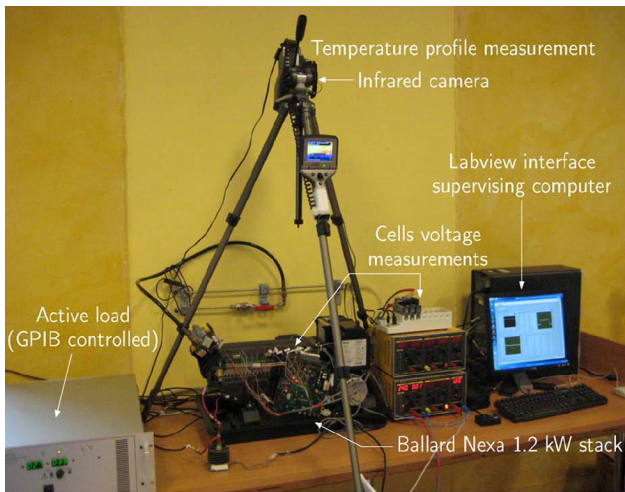


Fig. 2. NEXA Ballard 1.2 kW fuel cell stack experimental platform.

Table 2
Nexa Ballard fuel cell operating condition.

	Group 1	Group 2	Group 3	Group 4
Operating hours	400 h			
Number of cells	47			
Air supply	Air blower & filter			
Cooling system	Air fan cooled			
Fuel gas supply	99.99% dry H ₂ @1.2 bar			
Operating mode	Dead-end mode			
Air stoichiometry	4.2	2.2	2.0	2.0
Stack temperature	30 °C	35 °C	40 °C	44 °C
Current density	0.08 A/cm ²	0.20 A/cm ²	0.24 A/cm ²	0.30 A/cm ²

Table 3
PM200 fuel cell operating condition.

	Group 5	Group 6	Group 7	Group 8
Air supply	Air blower & filter			
Cooling system	DI-water/glycol			
Fuel gas supply	99.99% dry H ₂ @1.5 bar			
Number of cells	5	5	96	96
Operating hours	1000 h	1000 h	10500 h	450 h
Operating mode	Dy. load	Con. load	Con. load	Dy. load
Stack temp.	60 °C	60 °C	58 °C	58 °C
Current density	0.63–0.77 A/cm ²	0.70 A/cm ²	0.64 A/cm ²	0.2–0.99 A/cm ²

2.2.2. Proto Motor 200 fuel cell

Another group of aging experiments is conducted on the Proton Motor 200 1 kW and 25 kW fuel cells. As shown in Fig. 3, the cyclic load tests on the PM200 PEMFC are realized by the fuel cell experimental test platform. In this group of experiments, different PM200 PEMFCs with 96 cells and 5 cells are tested under various operating conditions as summarized in the Table 3. The fuel cell is operated under a constant temperature, 58 °C and 60 °C respectively, with pure 1.5 bar dry H₂ as input fuel. Two PM200 fuel cells with 5 cells are tested for 1000 h under dynamic load (group 5) and 1000 h under constant load (group 6) operating, respectively. Another two PM200 fuel cells with 96 cells are tested for 10,500 h under constant load (group 7) and 450 h under dynamic load (group 8) operating, respectively.

Specifically, in order to simulate the operating condition for fuel cell applied to variable loads, dynamic load tests are implemented to the PM200 fuel cells aging tests, and the corresponding dynamic current profile and output voltage are recorded. As shown in Fig. 4, the measured fuel cell current cycled from 20 A to 70 A and 100 A in 24 h in order to satisfy varies load requirements for group 8. Once the step current change is applied to the fuel cell, the output voltage responds with a first-order dynamic response curve.

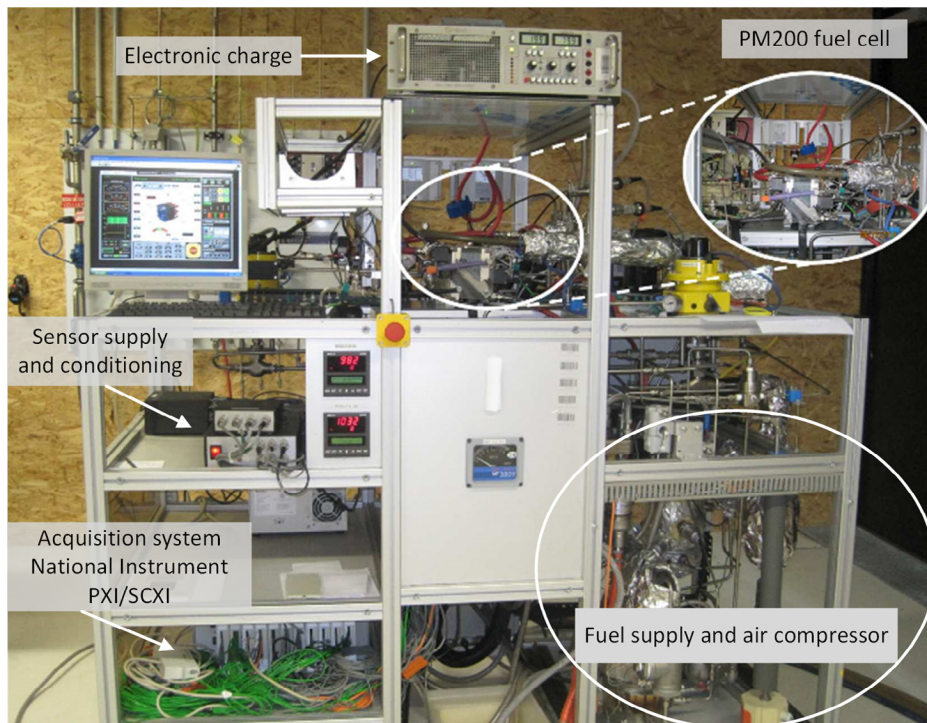


Fig. 3. Proton Motor fuel cell stack experimental platform.

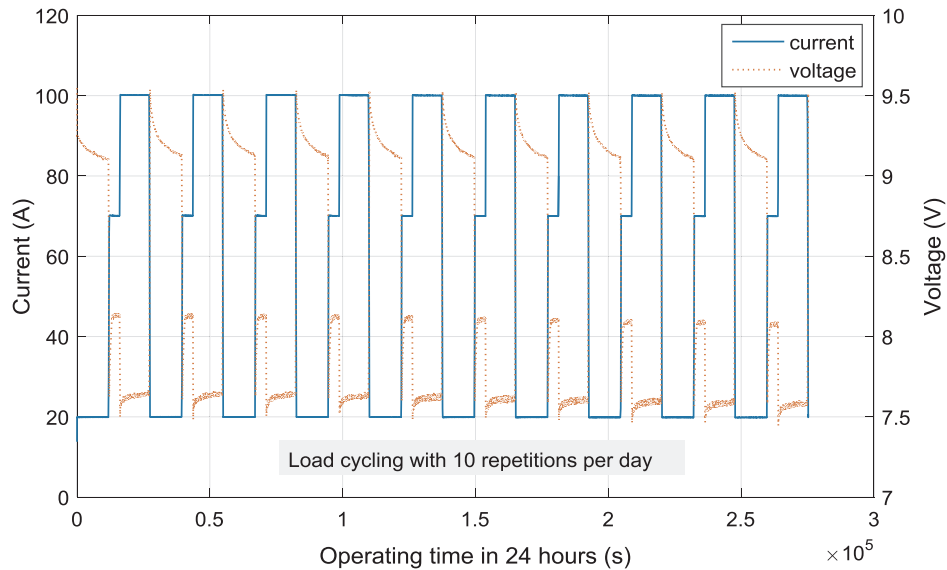


Fig. 4. Experimental measured output current and voltage (group 8).

3. Deep learning by grid long short-term memory network

In this section, the grid LSTM network for fuel cell degradation predication will be developed. Deep learning architectures like RNN have been successfully applied to research fields including computer vision, speech recognition and time series forecasting. Since fuel cell degradation prediction needs to deal with high non-linear characteristics of the fuel cell during a long-time period, the LSTM architecture can also be used instead of the conventional RNN.

3.1. RNN by LSTM architecture

Feedforward networks are amnesiacs regarding their recent past, and they remember nostalgically only the formative moments of training [39]. Similar with the commonly used feedforward network, three layers are taken into consideration for a traditional RNN as shown in Fig. 5(a): input layer, hidden layer and output layer. However, the difference between RNN and feedforward network can be distinguished by the self-recurrent connection of the neurons: the input of RNN neurons is not just the current input, but also what they have perceived previously in time.

Although RNN has “memory” to improve the performance, vanishing/exploding gradient problems are emerged as a major obstacle for its application in long time series forecasting [39]. During the gradient back-propagation phase of RNN, the gradient signal can end up being multiplied many times by the weight matrix associated with the connections between the neurons of the recurrent hidden layer. Once the

eigenvalue of the weight matrix is smaller than 1.0, the gradient signal will become too small to learn data in long-term time dependencies. This phenomenon is known as gradient vanishing. Whereas if the eigenvalue is larger than 1.0, exploding gradients will happen since the gradient signal is too large.

Specifically, the formula of the error δ_k^T to backpropagation through time (BPTT) can be expressed as [40]:

$$\delta_k^T = \delta_t^T \prod_{i=k}^{t-1} \text{diag}[f'(\text{net}_i)] W \quad (2)$$

where δ is the error for each neurons, W is the weight matrix of the self-recurrent connection, and net_i is weighted input for the neuron.

By evaluating the numerical value of every term in δ_k^T , the norm of the upper bound can be obtained as:

$$\|\delta_k^T\| \leq \|\delta_t^T\| \prod_{i=k}^{t-1} \|\text{diag}[f'(\text{net}_i)]\| \|W\| \leq \|\delta_t^T\| \beta_f \beta_W^{t-k} \quad (3)$$

where β_f and β_W are norm of the upper bound for diagonal matrix $\text{diag}[f'(\text{net}_i)]$ and weight matrix W , respectively.

It can be seen from (3) that when error is passed from time point t to time point k , the upper bound of its value is an exponential function of $\beta_f \beta_W$. Thus, when $t-k$ is very large (error been passed for a long time period), the value of (3) will be extremely small ($\beta_f \beta_W < 1$) or large ($\beta_f \beta_W > 1$), which correspond to the above mentioned gradient vanishing and exploding problem, respectively.

These issues are the main motivation behind the LSTM model which introduces a new structure called a LSTM cell as shown in Fig. 5(b). Despite of the self-recurrent connection neuron, an input gate, a forget gate and an output gate are added compared with conventional RNN architecture. By replacing each RNN neurons in the hidden layer to the LSTM memory cell, the LSTM based RNN can be obtained.

The self-recurrent connection in LSTM cell are designed in order to modulate the interactions between the cells themselves and their environment. By setting the weight of the self-recurrent neurons to 1.0, the state of a LSTM cell can remain constant. According to the training requirement, the forget gate can influence the recurrent connection by allowing the LSTM cell to remember or forget the state of previous step. Meanwhile, if the signal data are fed from the input gate, the current state of the cell can be modified. By filtering the output data, the output gate can decide whether the influence to other neurons is needed.

In order to explain the LSTM cell in a mathematical programming way, a flowchart is shown in Fig. 6. The horizontal flow path at the

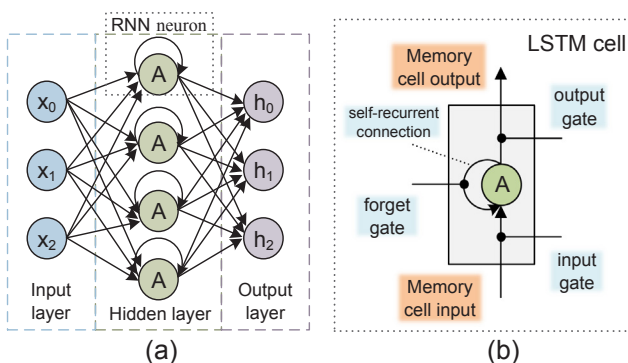


Fig. 5. RNN example and an LSTM memory cell.

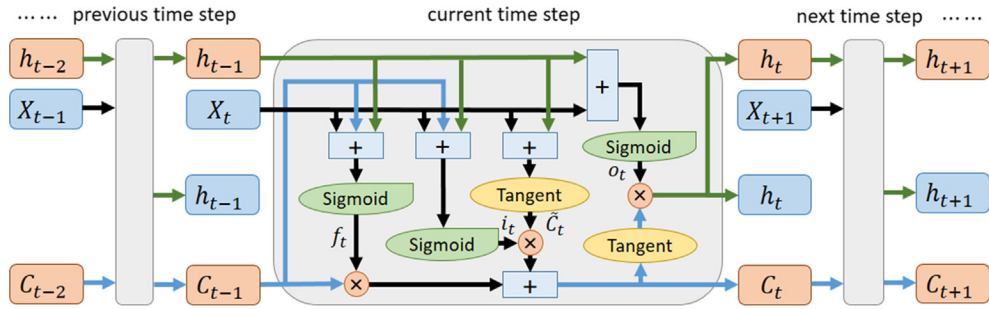


Fig. 6. Architecture of the LSTM memory cell.

bottom can preserve the needed training data information in a long time period through the network cell state, which is the key to the LSTM RNN. The cell state need to be updated at every time step, and X_t stands for the input of the current time step, h_t and h_{t-1} are the output from current and previous time step, respectively, C_t and C_{t-1} are the memory of the current and previous time step.

First, the mathematical definition of gate can be expressed as:

$$g(x) = \sigma(Wx + b) \quad (4)$$

Then, the numerical value of the input gate layer for current time step can be obtained as:

$$i_t = \sigma[W_i \cdot (X_t, h_{t-1}, C_{t-1}) + b_i] \quad (5)$$

Meanwhile, the candidate value \tilde{C}_t are created to be added to the state as:

$$\tilde{C}_t = \tanh[W_C \cdot (X_t, h_{t-1}) + b_C] \quad (6)$$

The above-mentioned i_t and \tilde{C}_t creates an update to the cell state. By considering the calculation of forget gate layer as:

$$f_t = \sigma[W_f \cdot (X_t, h_{t-1}, C_{t-1}) + b_f] \quad (7)$$

The updated cell state can be expressed as:

$$C_t = f_t \circ C_{t-1} + i_t \circ \tilde{C}_t \quad (8)$$

Finally, the output gate layer decide which part of the state can be obtained based on cell state as:

$$\begin{cases} o_t = \sigma[W_o \cdot (X_t, h_{t-1}) + b_o] \\ h_t = o_t \circ \tanh(C_t) \end{cases} \quad (9)$$

where $\sigma(z)$ is the activation function, $\tanh(z)$ is the output function, W_f , W_i , W_o and W_C are the weight matrices, b_f , b_i , b_o and b_C are bias vectors, \circ means multiplied by the elements (for more details, please refer to the Appendix A).

3.2. Grid LSTM architecture

It can be seen from the architecture of the traditional LSTM cell that, the network can be easily connected between different time steps. Thus, a grid LSTM is developed based on the paralleling and combining of individual LSTM cells. As shown in Fig. 7, despite the memory of time, two-dimensional (2D) grid LSTM (G-LSTM) architecture also shows the ability of the memory for depth. By adding LSTM cells along the depth dimension of the network, the memory for both the time and depth can be obtained at the same time [40]. Each layer uses both a hidden state and a memory cell to communicate with others, which makes the depth dimension has the same gradient channeling properties with the temporal dimension. Thus, the G-LSTM can allow the individual layer to remember or ignore their inputs, which can efficiently mitigate the vanishing gradient problem in multi-layer networks as mentioned in the previous section.

For fuel cell degradation phenomenon, a deeper network and a simple architecture can make the prognostic to be possibly executed

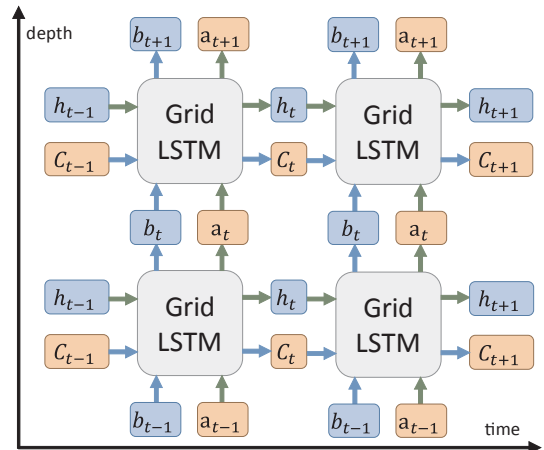


Fig. 7. 2D Grid LSTM architecture.

online, which can help to predict in real-time the fuel cell lifetime. In addition to the fuel cell output voltage data (electrical domain), other measured data such as fuel cell temperature (thermal domain) can also help to indicate the degradation. Thus, with 2D G-LSTM or even a higher dimensional (3D) LSTM, deeper network can be applied for the training data to achieve a better prediction precision.

3.3. Implementation for degradation predication

With the G-LSTM architecture introduced in the previous section, the fuel cell degradation prediction model is developed through training the G-LSTM network. The training framework for PEMFC performance degradation model is shown in Fig. 8. On the right side of the figure shows the complete G-LSTM RNN training algorithm, which includes four major steps:

1. Forward propagation of each neurons' output. For G-LSTM proposed in this work, this step means the calculation of five vectors including f_t , i_t , C_t , o_t and h_t .
2. Back propagation of error for each neuron. Similar with traditional RNN, the error will back propagation through two directions. One is along the opposite direction of time line, which means calculating the error at every time step form the current time step. Another direction is the propagation to the previous network layer.
3. Calculation of gradient for every weight according to corresponding error term. (More details related to the calculation of error and gradient terms are demonstrated in the Appendix A)
4. Update weight through stochastic gradient decent method.

In addition to the network training, some additional data processing are also necessary for the development of our proposed fuel cell degradation prediction model. As mentioned before, the experimentally measured data such as fuel cell current, output voltage, temperature are

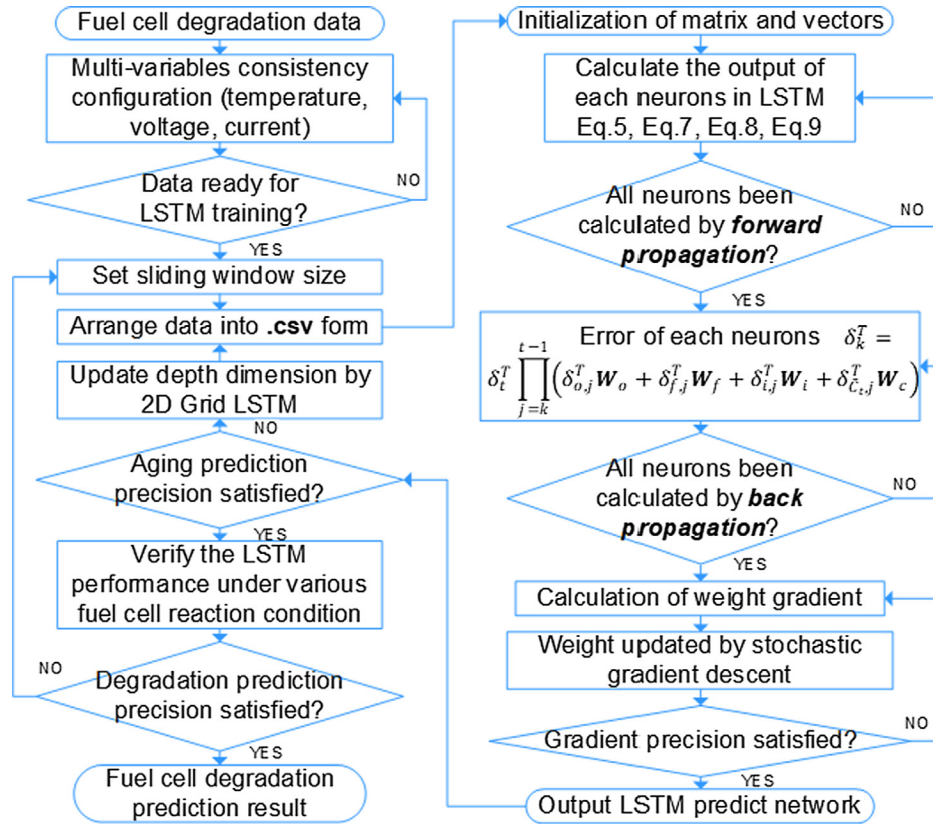


Fig. 8. Training process of fuel cell degradation prediction model.

collected and the ripples needs to be removed. Other experimental data like fuel gas pressure and temperature at the inlet and outlet part of the fuel cell can also help the formation of a deeper LSTM RNN. Moreover, as shown in Fig. 9, another essential part of the training process is the update of the sliding window size for trained data. During the recurrent network training process, the data is used for training and verifying step by step. The prediction of the next time step value depends not only on previous one time step, but also on the value of many steps before. Thus, once the target prediction network fails to meet the required prediction precision, the sliding window size can be updated to be able to maintain the prediction accuracy.

4. Deep learning prediction results and discussions

In this section, the fuel cell performance prediction results using our proposed deep learning approach are demonstrated by the trained grid LSTM network. The prediction performance for both long-time and short-time period are discussed and compared with the experimental measured data. Moreover, a relevance vector machine and other conventional RNNs are deployed to make the comparisons with proposed G-LSTM RNN.

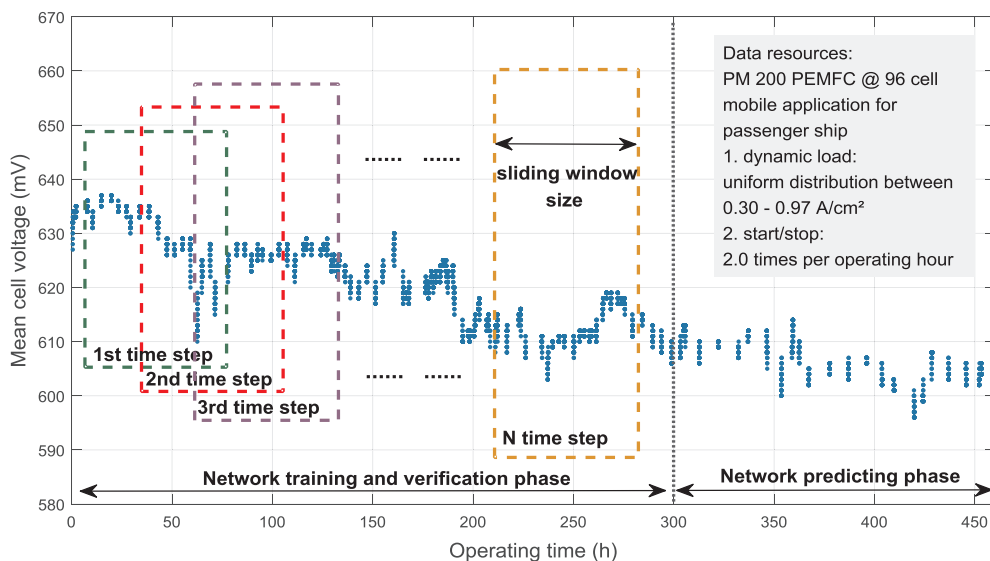


Fig. 9. Sliding window size update for the training data of LSTM RNN.

4.1. Prediction performance criteria

The performance of the prediction model can be evaluated by the three commonly used criteria including the mean absolute percentage error (MAPE), the root-mean-square error (RMSE) and the coefficient of determination (R^2). Smaller values of MAPE and RMSE indicate more accurate prediction with lower errors. Different from MAPE and RMSE, a larger value of R^2 indicate a better prediction, and $R^2 = 1$ if the prediction fit the experimental data perfectly. The equations for those criteria can be expressed as:

$$\text{MAPE} = \frac{1}{N} \sum_1^N \frac{|X(t) - \hat{X}(t)|}{|X(t)|} \quad (10)$$

$$\text{RMSE} = \sqrt{\frac{1}{N} \sum_1^N (X(t) - \hat{X}(t))^2} \quad (11)$$

$$R^2 = 1 - \frac{\sum_1^N (X(t) - \hat{X}(t))^2}{\sum_1^N (X(t) - \bar{X}(t))^2} \quad (12)$$

where $X(t)$ represents the measured real voltage value, $\hat{X}(t)$ is the voltage value predicted by the degradation model, $\bar{X}(t)$ indicates the average value of the voltage data, N is the number of the measured voltage values.

4.2. Degradation prediction results for Ballard NEXA fuel cell

The aging data of Ballard NEXA PEMFCs are first used to train the LSTM RNN and to validate the prediction results. The predicted results are compared with the RVM degradation predicting results reported in [19,20]. As shown in Fig. 10(a)–(d), four data sets under different fuel cell aging operating conditions are deployed (group 1 to group 4). The voltage data from 0 h to 240 h are used to train the network, and the rest are used to verify the prediction accuracy. In this groups of validation, the sliding window size is set to 5, the delay layer is 2 and hidden neuron number is 10.

It should be noticed that the distributions of training data from the first two group have a larger variation when compared with the rest two groups. The reason is due to the fuel cell temperature variation. For NEXA system, the cooling of the fuel cell is realized through a controlled fan, which has a minimum speed. However, the embedded control algorithm makes the fan work intermittently when the fuel cell operates with a lower current, which is the reason why the output voltage of the fuel cell varies a lot. When the fuel cell temperature is relative lower, the fan will stop working. Then the temperature will increase, and the fan will re-start to work since the temperature is relative higher. Since the fuel cell currents of group 1 and group 2 are only 12 A and 30 A, there is no need for the continuous operation of the fan. It can also be noticed that the variation for group 1 happens not only in the training data, but also in the test data due to the lower operating current.

Specially, for fuel cell degradation with 12 A output current under operating temperature of 30 °C, the MAPE decreases from 0.0052 to 0.0047, which corresponds with the training and prediction phase, respectively. The determination coefficients R^2 are around 0.85 for this group. Compared to the training part, the voltage curve of prediction test part is smoother. Meanwhile, compared to the RVM approach, the LSTM based approach can reach a much higher precision. By increasing the fuel cell current form 12 A to 30 A, and the temperature form 30 °C to 35 °C, the LSTM based approach can have a smoother predicting results curve on the prediction phase. In this group test, the MAPE for both training and prediction phase decreases, and the training outputs are much smoother than previous group 1 operating condition. The determination coefficients R^2 is around 0.93, which indicates the trained and predicted data fit the experimental data very well. Whereas for the RVM based model, the predicted voltage failed to capture the tendency around the points near to 400 h. If we continue to increase the fuel cell operating current to 40 A and 44 A, a clear degradation can be

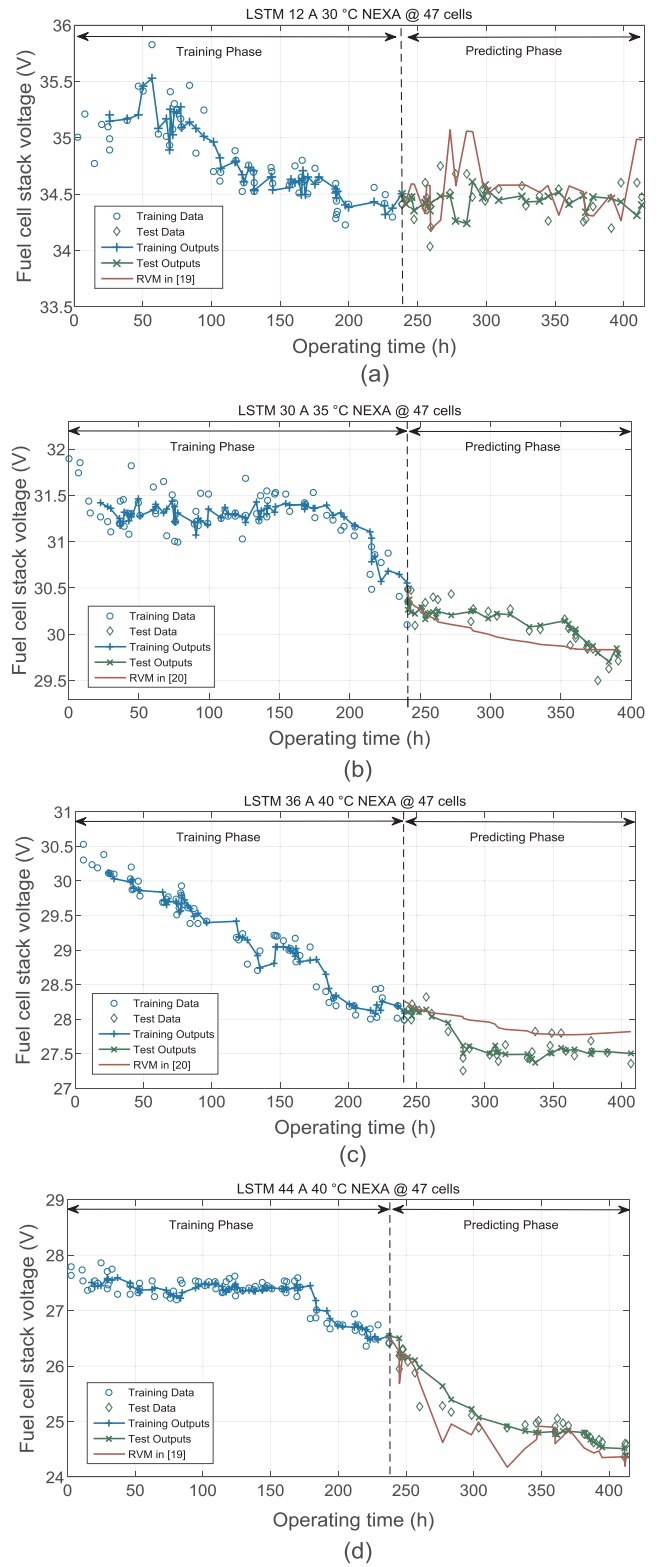


Fig. 10. LSTM RNN prediction curves for NEXA PEMFC.

observed by the decreasing output voltage value under 40 °C. The trained LSTM RNN shows very good result for the prediction of these two group tests. The overall MAPE is around 0.0040, and the determination coefficients R^2 are all over 0.95. Especially for group 4, the training outputs and predicted output fit the experimental very well, and RMSE of the prediction even reach 0.9848. The RVM based degradation model can have a better performance on the prediction for

Table 4
Error assessment for NEXA PEMFC.

	Group 1 (12 A 30 °C)		Group 2 (30 A 35 °C)	
	Train	Test	Train	Test
MAPE	0.0052	0.0047	0.0036	0.0034
RMSE	0.1719	0.1667	0.1410	0.1395
R ²	0.8644	0.8458	0.9354	0.9456
	Group 3 (36 A 40 °C)		Group 4 (44 A 40 °C)	
	Train	Test	Train	Test
MAPE	0.0038	0.0040	0.0042	0.0041
RMSE	0.1487	0.1513	0.1618	0.1041
R ²	0.9719	0.9747	0.9581	0.9848

group 3, whereas the required predicting accuracy for group 4 could not be reached.

The overall error assessment can be obtained in **Table 4**. The LSTM short-term prediction accuracy is proved by the experimental validation data, indicating the effectiveness of the proposed degradation model. However, we should also notice that the distribution of the training data can strongly influence the prediction performance since both the training outputs for group 1 and group 2 varies a lot. We can thus conclude that the model performance for group 3 and group 4 is better than the first two group. This corresponding to the fact that the prediction is more reliable under a uniform distributed training data.

4.3. Degradation prediction results for PM200 fuel cell

In order to better explore the short-term and long-term prediction performance of the proposed G-LSTM fuel cell degradation RNN, another group of experimental data of PM200 PEMFC are used and discussed in this section.

4.3.1. Performance for short-term aging

The data from group 5 and group 6 are used to train and test the model short-term aging performance. **Fig. 11(a)** gives the comparison between the LSTM and 2D G-LSTM predictive results. The first 690 h among the 1000 h measurement data are used to train the model, and the rest are used to verify the prediction performance. By setting the delay layer to 2 and hidden neuron numbers L to 10, the performance of G-LSTM is better than LSTM under both constant and dynamic load degradation operating conditions. It can be seen from the figure that, the LSTM loses the data traction at the ripple parts of the voltage degradation curve and shows a lower accuracy for predicting data fittings, whereas the G-LSTM can follow the degradation trend despite of those ripples and can reach a higher accuracy at the prediction phase. In order to check specifically the G-LSTM model performance, error analysis is conducted and presented in **Fig. 11(b)** and (c).

As can be seen from **Fig. 11(b)**, the overall degradation trend of the fuel cell under dynamic load input are influenced by the voltage recovery phases (nonlinear voltage increases at low load cycle). However, the G-LSTM can still capture the degradation trend very well. For the training phase, most of the errors between training targets and outputs are within 0.02 V, which indicate that the network learned the data in a

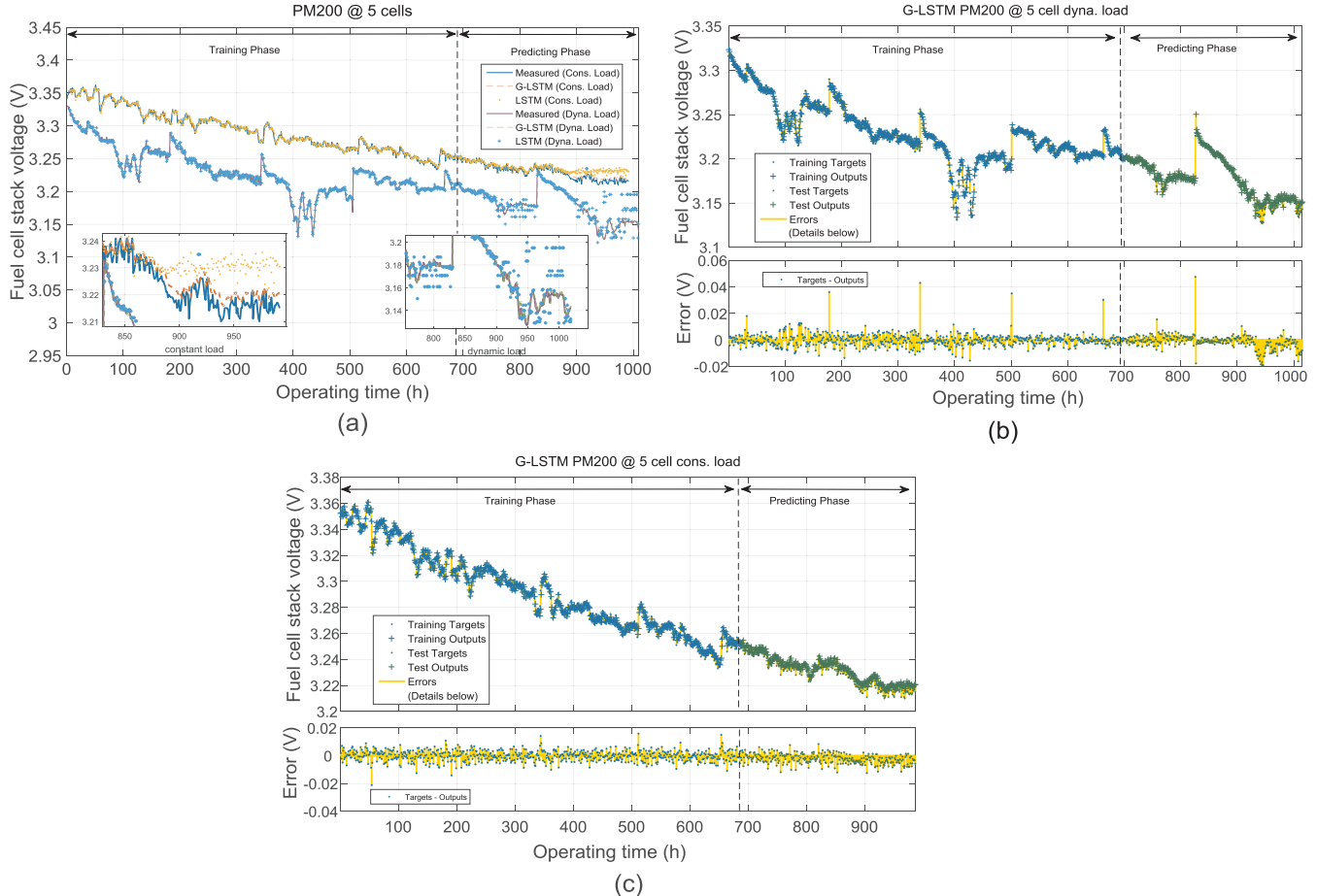


Fig. 11. Degradation prediction curves for PM200 PEMFC (5 cells).

Table 5
Error assessment for PM200 PEMFC.

	Group 5		Group 6	
	Train	Test	Train	Test
MAPE	0.0010	0.0013	0.0017	0.0018
RMSE	0.0054	0.0050	0.0039	0.0040
R ²	0.9872	0.9919	0.9951	0.9923

precise way. For the prediction phase, the biggest error is about 0.05 V, which occurs when the voltage degradation curves face a nonlinear increase (voltage recovery). The RMSE for training and predicting phase are 0.0049 and 0.0052, respectively. Compared with the NEXA fuel cell prediction, the model performance improves a lot. This is because a bigger dataset can be more suitable for the deep learning, and the trained model can thus make prediction effectively. The coefficient of determination R² come to be 0.9936 and 0.9917, respectively, which indicate the good performance for the proposed G-LSTM degradation prediction model.

A more obvious degradation tendency of the fuel cell voltage can be observed in Fig. 11(c). This group test is for fuel cell operating under 70A constant current for 1000 h. For this dataset, the proposed G-LSTM network also performs well on the entire operating time range. The training output fit the training data with a RMSE of 0.0048, and the predicting outputs RMSE is 0.0050. For the error distributions, the training phase are all within 0.05 V and the prediction phase are within 0.04 V. It can be concluded that, the G-LSTM degradation model can achieve a high fuel cell aging prediction accuracy. The error assessment are summarized in Table 5.

4.3.2. Performance for long-term aging

Long-term polarization performance of fuel cell can indicate the fuel cell lifetime, and a precise degradation prediction can help to develop

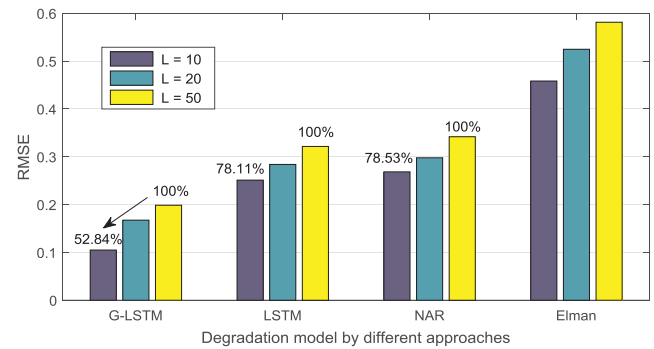


Fig. 13. RMSE analysis for PM200 PEMFC (96 cells).

the prognostic and diagnostic control methods. In this section, the experimental measured data from group 7 are used to verify the G-LSTM performance applied in long-term performance degradation prediction as shown in Fig. 12. The training data come from the first 6100 h of the dataset, and the rest are used to verify the prediction results.

By setting the hidden neurons L to 10, the degradation predicted by LSTM and G-LSTM are first compared in the Fig. 12(a). Under the same model training condition, the G-LSTM shows better prediction results by predicting the test voltage measurement data in a precise way. The average error of the LSTM approach is around 10 mV at the prediction phase and the error for G-LSTM approach is within 3 mV. For the training phase, the G-LSTM approach can follow the training data on the entire range, whereas the LSTM approach shows a divergence tendency at the end part of the training data. Moreover, the error of LSTM at predicting phase gradually increases whereas the error of G-LSTM remains to be stable.

Fig. 12(b) compares the predicting performance between the proposed G-LSTM approach and non-linear autoregressive (NAR) neural network. It can be noticed that, a larger number of hidden neurons for

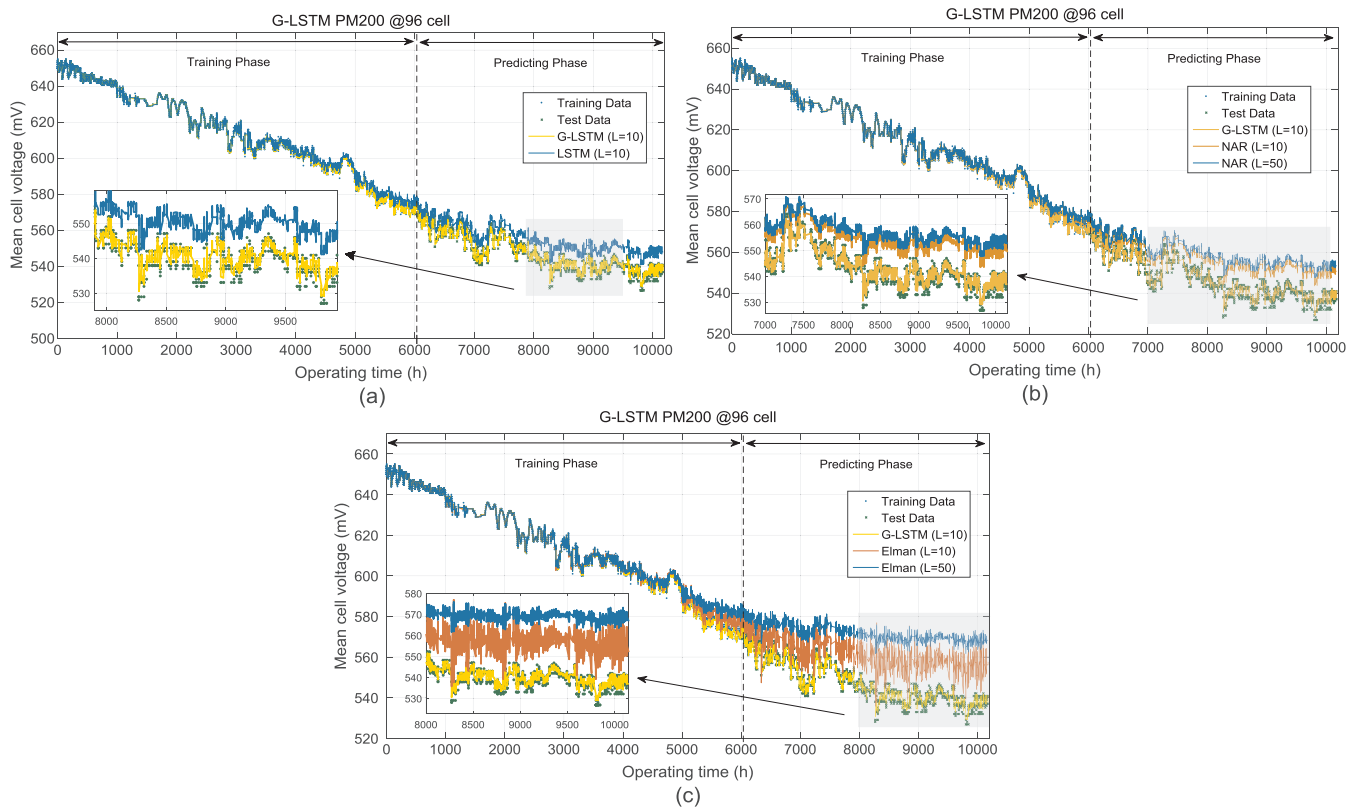


Fig. 12. Degradation prediction curves for PM200 (constant load, 96 cells).

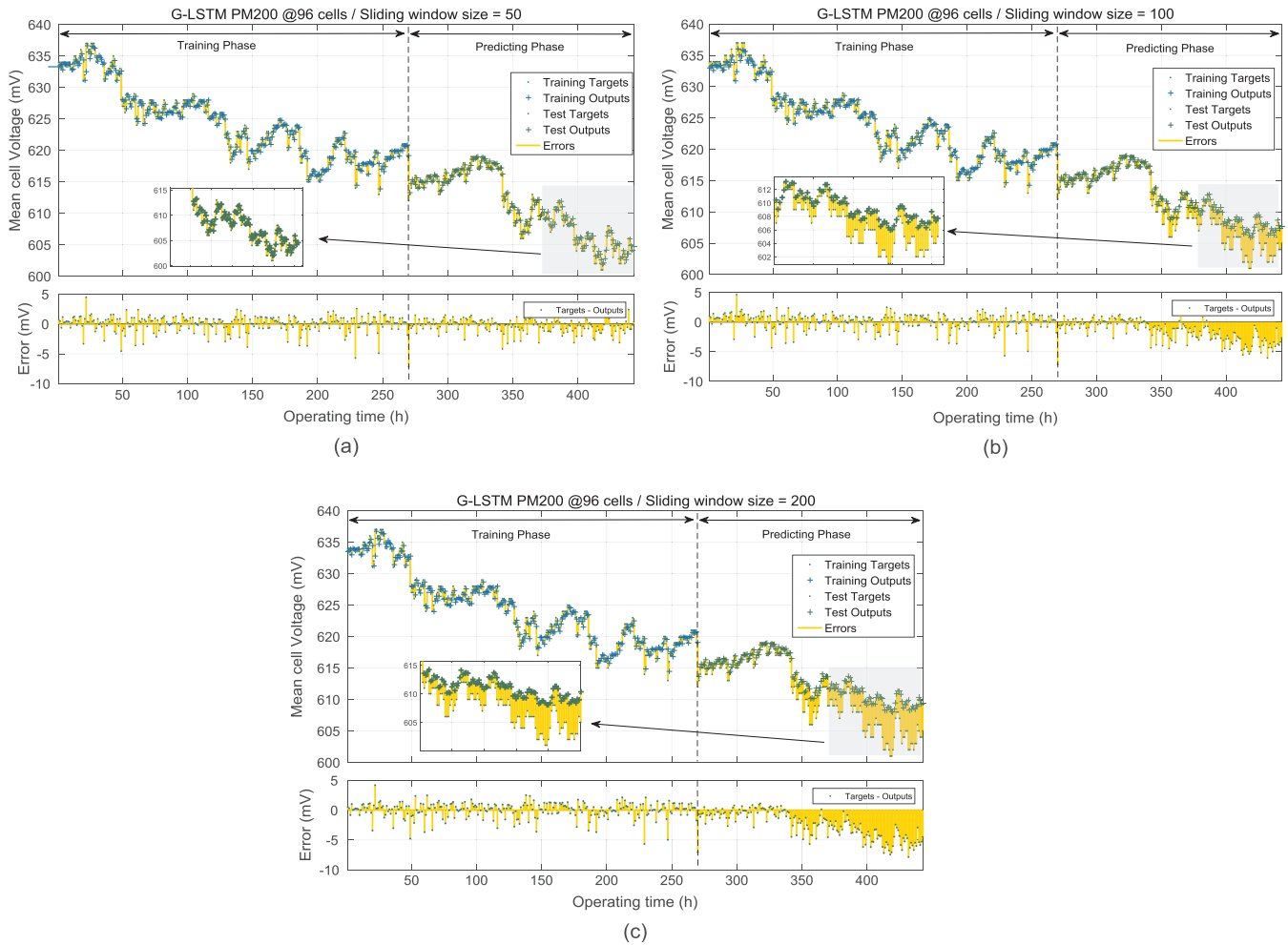


Fig. 14. Degradation prediction curves for PM200 (dynamic load, 96 cells).

NAR lead to a lower prediction accuracy. For 10 hidden neurons setting of the network, G-LSTM shows an obviously higher accuracy. The errors of NAR approach are near 20 mV at the end part of the predicting phase, whereas G-LSTM approach, as mentioned above, are within 3 mV. Meanwhile, compared with LSTM approach in Fig. 12(a), the data divergence between training outputs and measured data of NAR approach appears earlier. At last, the performance of Elman network is compared with the proposed G-LSTM in Fig. 12(c). The results show that, for this fuel cell degradation dataset, a larger neuron numbers indicates a larger prediction error, which has been verified in Fig. 12(b). Moreover, the prediction error of the Elman approach is over 30 mV at the prediction phase. The oscillation of the prediction results is very large and appears earlier than all previous mentioned approaches.

The RMSE distribution for different long-term fuel cell aging prediction approaches are shown in Fig. 13. Different training settings for the hidden neuron numbers are deployed to the network training, and LSTM based approaches perform obviously better than the other two approaches. We can conclude that for fuel cell long-term degradation prediction, G-LSTM can effectively track the voltage drop trend and predict the fuel cell performance degradation.

4.3.3. Performance under varies sliding window size

In this part, G-LSTM networks performance under different sliding window sizes are further analyzed in order to discuss its influence on the prediction accuracy. The dataset from group 8 is measured under a dynamic load operating condition, which includes many voltage

oscillations in the degradation curve. The training and predicting results are demonstrated in Fig. 14.

As can be seen from Fig. 14(a)–(c), the sliding window sizes change from 50 to 100 and 200. It can be concluded from the figures that, a smaller window size can lead to smaller training and predicting errors. When the training window size is set to 50, all the errors of the predicting phase in Fig. 14(a) are within 5 mV. However, when we increase the window size to 100, the error becomes larger at the predicting phase, and there are 6 data points over than 5 mV. At last, the window size of 200 results to lots of larger error points over than 5 mV. However, the errors of the training targets output are not influenced by the sliding window sizes variation. Based on this group tests, we can conclude that the sliding windows size should not be too large compared with total time steps.

5. Conclusion

This paper proposed a novel data-driven deep learning fuel cell degradation prognostic model, using recurrent neural network (RNN) with grid long short-term memory (G-LSTM) cell in order to avoid gradient vanishing or exploding problem in the network training. Both the long-term and short-term fuel cell aging experiments are conducted using different PEMFCs. The model prediction results are validated with eight different load profiles from eight different fuel cells (three types). Meanwhile, Different degradation models including RVM model, NAR network and Elman network are compared with the proposed G-LSTM one. The conclusion can be made as follows:

1. The results indicate that the proposed G-LSTM model can effectively reach a high prediction accuracy under varied fuel cell operating conditions, with voltage prediction achieving a RMSE of 0.0040 and a MAPE of 0.0013.
2. The track for the large output variation can be obtained through the proposed model, whereas the prognostic model can have a better performance and be more reliable compared to the existing works when the training data have small variations.
3. The prediction model performance tested under varied sliding window sizes can help to design the training criteria of data-based fuel cell aging model.
4. The proposed data-driven model can fit different fuel cells degradation within the same training framework.

Appendix A

The gate activation function and output activation function can be expressed as:

$$\sigma(z) = y = \frac{1}{1 + e^{-z}}, \sigma'(z) = y(1-y) \quad (A.1)$$

$$\tanh(z) = y = \frac{e^z - e^{-z}}{e^z + e^{-z}}, \tanh'(z) = 1 - y^2 \quad (A.2)$$

Define operate \circ as multiplied by the elements:

$$a \circ b = \begin{bmatrix} a_1 \\ a_2 \\ a_3 \\ \dots \\ a_n \end{bmatrix} \circ \begin{bmatrix} b_1 \\ b_2 \\ b_3 \\ \dots \\ b_n \end{bmatrix} = \begin{bmatrix} a_1 b_1 \\ a_2 b_2 \\ a_3 b_3 \\ \dots \\ a_n b_n \end{bmatrix} \quad (A.3)$$

$$a \circ X = \begin{bmatrix} a_1 \\ a_2 \\ a_3 \\ \dots \\ a_n \end{bmatrix} \circ \begin{bmatrix} x_{11} & x_{12} & x_{13} & \dots & x_{1n} \\ x_{21} & x_{22} & x_{23} & \dots & x_{2n} \\ x_{31} & x_{32} & x_{33} & \dots & x_{3n} \\ \dots & \dots & \dots & \dots & \dots \\ x_{n1} & x_{n2} & x_{n3} & \dots & x_{nn} \end{bmatrix} = \begin{bmatrix} a_1 x_{11} & a_1 x_{12} & a_1 x_{13} & \dots & a_1 x_{1n} \\ a_2 x_{21} & a_2 x_{22} & a_2 x_{23} & \dots & a_2 x_{2n} \\ a_3 x_{31} & a_3 x_{32} & a_3 x_{33} & \dots & a_3 x_{3n} \\ \dots & \dots & \dots & \dots & \dots \\ a_n x_{n1} & a_n x_{n2} & a_n x_{n3} & \dots & a_n x_{nn} \end{bmatrix} \quad (A.4)$$

The error term at time step t δ_t can be expressed as:

$$\delta_t = \frac{\partial E}{\partial h_t} \quad (A.5)$$

The error backward pass along backpropagation, thus the error term at time step t - 1 δ_{t-1} can be expressed as:

$$\delta_{t-1} = \delta_{o,t}^T \frac{\partial net_{o,t}}{\partial h_{t-1}} + \delta_{f,t}^T \frac{\partial net_{f,t}}{\partial h_{t-1}} + \delta_{i,t}^T \frac{\partial net_{i,t}}{\partial h_{t-1}} + \delta_{\tilde{c},t}^T \frac{\partial net_{\tilde{c},t}}{\partial h_{t-1}} = \delta_{o,t}^T \mathbf{W}_o + \delta_{f,t}^T \mathbf{W}_f + \delta_{i,t}^T \mathbf{W}_i + \delta_{\tilde{c},t}^T \mathbf{W}_{\tilde{c}} \quad (A.6)$$

where,

$$\delta_{o,t}^T = \delta_t^T \circ \tanh(c_t) \circ o_t \circ (1-o_t) \quad (A.7)$$

$$\delta_{f,t}^T = \delta_t^T \circ o_t \circ (1-\tanh(c_t)^2) \circ c_{t-1} \circ f_t \circ (1-f_t) \quad (A.8)$$

$$\delta_{i,t}^T = \delta_t^T \circ o_t \circ (1-\tanh(c_t)^2) \circ \tilde{c}_t \circ i_t \circ (1-i_t) \quad (A.9)$$

$$\delta_{\tilde{c},t}^T = \delta_t^T \circ o_t \circ (1-\tanh(c_t)^2) \circ i_t \circ (1-\tilde{c}_t^2) \quad (A.10)$$

Thus, we can obtain the equation for passing forward the error term to any time step k as:

$$\delta_k^T = \prod_{j=k}^{t-1} \delta_{o,j}^T \mathbf{W}_o + \delta_{f,j}^T \mathbf{W}_f + \delta_{i,j}^T \mathbf{W}_i + \delta_{\tilde{c},j}^T \mathbf{W}_{\tilde{c}} \quad (A.11)$$

Then the weight gradient at time step t can be obtained as:

$$\frac{\partial E}{\partial \mathbf{W}_{o,t}} = \frac{\partial E}{\partial net_{o,t}} \frac{\partial net_{o,t}}{\partial \mathbf{W}_{o,t}} = \delta_{o,t} h_{t-1}^T \quad (A.12)$$

$$\frac{\partial E}{\partial \mathbf{W}_{f,t}} = \frac{\partial E}{\partial net_{f,t}} \frac{\partial net_{f,t}}{\partial \mathbf{W}_{f,t}} = \delta_{f,t} h_{t-1}^T \quad (A.13)$$

$$\frac{\partial E}{\partial \mathbf{W}_{i,t}} = \frac{\partial E}{\partial net_{i,t}} \frac{\partial net_{i,t}}{\partial \mathbf{W}_{i,t}} = \delta_{i,t} h_{t-1}^T \quad (A.14)$$

$$\frac{\partial E}{\partial \mathbf{W}_{\tilde{c},t}} = \frac{\partial E}{\partial \text{net}_{\tilde{c},t}} \frac{\partial \text{net}_{\tilde{c},t}}{\partial \mathbf{W}_{c,t}} = \delta_{\tilde{c},t} h_{t-1}^T \quad (\text{A.15})$$

The final gradient for weight matrixes can be expressed as:

$$\frac{\partial E}{\partial \mathbf{W}} = \sum_{j=1}^t \delta_j h_{t-1}^T \quad (\text{A.16})$$

Similar, the gradient for bias vectors can be obtained as:

$$\frac{\partial E}{\partial \mathbf{b}_{o,t}} = \frac{\partial E}{\partial \text{net}_{o,t}} \frac{\partial \text{net}_{o,t}}{\partial \mathbf{b}_{o,t}} = \delta_{o,t} \quad (\text{A.17})$$

$$\frac{\partial E}{\partial \mathbf{b}_{f,t}} = \frac{\partial E}{\partial \text{net}_{f,t}} \frac{\partial \text{net}_{f,t}}{\partial \mathbf{b}_{f,t}} = \delta_{f,t} \quad (\text{A.18})$$

$$\frac{\partial E}{\partial \mathbf{b}_{i,t}} = \frac{\partial E}{\partial \text{net}_{i,t}} \frac{\partial \text{net}_{i,t}}{\partial \mathbf{b}_{i,t}} = \delta_{i,t} \quad (\text{A.19})$$

$$\frac{\partial E}{\partial \mathbf{b}_{\tilde{c},t}} = \frac{\partial E}{\partial \text{net}_{\tilde{c},t}} \frac{\partial \text{net}_{\tilde{c},t}}{\partial \mathbf{b}_{c,t}} = \delta_{\tilde{c},t} \quad (\text{A.20})$$

And The final gradient for bias vector can be expressed as:

$$\frac{\partial E}{\partial \mathbf{b}} = \sum_{j=1}^t \delta_j \quad (\text{A.21})$$

References

- [1] Jahnke T, Futter G, Latz A, Malkow T, et al. Performance and degradation of proton exchange membrane fuel cells: state of the art in modeling from atomistic to system scale. *J Power Sources* 2016;304:207–33.
- [2] Breaz E, Gao F, Miraoui A, Tirnovan R. A short review of aging mechanism modeling of proton exchange membrane fuel cell in transportation applications. In: Proc. IEEE Ind. Electron. Soc.; 2014. p. 3941–3947.
- [3] Pei Pucheng, Chen Huicui. Main factors affecting the lifetime of Proton Exchange Membrane fuel cells in vehicle applications: a review. *Appl Energy* 2014;125:60–75.
- [4] Chandrisis M, Vincent R, Guetaz L, Roch J-S, Thoby D, Quinaud M. Membrane degradation in PEM fuel cells: from experimental results to semi-empirical degradation laws. *Int J Hydrogen Energy* 2017;42(12):8139–49.
- [5] Hu Z, Xu L, Li J, Ouyang M, Song Z, Huang H. A reconstructed fuel cell life-prediction model for a fuel cell hybrid city bus. *Energy Convers Manage* 2018;156:723–32.
- [6] Ozden E, Tari I. Proton exchange membrane fuel cell degradation: a parametric analysis using computational fluid dynamics. *J Power Sources* 2016;304:64–73.
- [7] Vasilyev A, Andrews J, Jackson LM, Dunnett SJ, Davies B. Component-based modelling of PEM fuel cells with bond graphs. *Int J Hydrogen Energy* 2017;42(49):29406–21.
- [8] Park Jaeman, Hwanyeong Oh, Ha Taehun, Lee Yoo Il, Min Kyoungdoug. A review of the gas diffusion layer in proton exchange membrane fuel cells: durability and degradation. *Appl Energy* 2015;155:866–80.
- [9] Chen Huicui, Pei Pucheng, Song Mancun. Lifetime prediction and the economic lifetime of proton exchange membrane fuel cells. *Appl Energy* 2015;142:154–63.
- [10] Urchaga P, Kadyk T, Rinaldo SG, Pistono AO, Hu J, et al. Catalyst degradation in fuel cell electrodes: accelerated stress tests and model-based analysis. *Electrochim Acta* 2015;176:1500–10.
- [11] Linder M, Hocker T, Meier C, Holzer L, et al. A model-based approach for current voltage analyses to quantify degradation and fuel distribution in solid oxide fuel cell stacks. *J Power Sources* 2015;288:409–18.
- [12] Jouin M, Bressel M, Morando S, Gouriveau R, Hissel D, Péra MC, et al. Estimating the end-of-life of PEM fuel cells: guidelines and metrics. *Appl Energy* 2016;1(177):87–97.
- [13] Javed K, Gouriveau R, Zerhouni N, Hissel D. Prognostics of Proton Exchange Membrane Fuel Cells stack using an ensemble of constraints based connectionist networks. *J Power Sources* 2016;30(324):745–57.
- [14] Ibrahim M, Steiner NY, Jemei S, Hissel D. Wavelet-based approach for online fuel cell remaining useful lifetime prediction. *IEEE Trans Ind Electron* 2016;63(8):5057–68.
- [15] Silva RE, Gouriveau R, Jemei S, Hissel D, Boulon L, Agbossou K, et al. Proton exchange membrane fuel cell degradation prediction based on adaptive neuro-fuzzy inference systems. *Int J Hydrogen Energy* 2014;39(21):11128–44.
- [16] Bressel Mathieu, Hilalret Mickael, Hissel Daniel, Bouamama Belkacem Ould. Extended Kalman filter for prognostic of proton exchange membrane fuel cell. *Appl Energy* 2016;164:220–7.
- [17] Jha MS, Bressel M, Bouamama BO, Ge D, Tanguy. Particle filter based hybrid prognostics of proton exchange membrane fuel cell in bond graph framework. *Comput Chem Eng* 2016;95:216–30.
- [18] Jouin M, Gouriveau R, Hissel D, Péra MC, Zerhouni N. Prognostics of PEM fuel cell in a particle filtering framework. *Int J Hydrogen Energy* 2014;39(1):481–94.
- [19] Wu Y, Breaz E, Gao F, Paire D, Miraoui A. Nonlinear performance degradation prediction of proton exchange membrane fuel cells using relevance vector machine. *IEEE Trans Energy Convers* 2016 Dec;31(4):1570–82.
- [20] Wu Y, Breaz E, Gao F, Miraoui A. A modified relevance vector machine for PEM fuel-cell stack aging prediction. *IEEE Trans Ind Appl* 2016;52(3):2573–81.
- [21] Zunyan Hu, Liangfei Xu, Huang Yiyuan, Li Jianqiu, Ouyang Minggao, Xiaoli Du, et al. Comprehensive analysis of galvanostatic charge method for fuel cell degradation diagnosis. *Appl Energy* 2018;212:1321–32.
- [22] Li Z, Outbib R, Hissel D, Giurgea S. Data-driven diagnosis of PEM fuel cell: a comparative study. *Control Eng Pract* 2014;1(28):1–2.
- [23] Li Z, Jemei S, Gouriveau R, et al. Remaining useful life estimation for PEMFC in dynamic operating conditions. In: IEEE Vehicle Power and Propulsion Conference (VPPC); 2016. p. 1–6.
- [24] Onanena R, Oukhellou L, Candusso D, Harel F, Hissel D, Aknin P. Fuel cells static and dynamic characterizations as tools for the estimation of their ageing time. *Int J Hydrogen Energy* 2011;36(2):1730–9.
- [25] Jung Guo-Bin, Chuang Kai-Yuan, Jao Ting-Chu, Yeh Chia-Chen, Lin Chih-Yuan. Study of high voltage applied to the membrane electrode assemblies of proton exchange membrane fuel cells as an accelerated degradation technique. *Appl Energy* 2012;100:81–6.
- [26] Liu H, Chen J, Hou M, Shao Z, Su H. Data-based short-term prognostics for proton exchange membrane fuel cells. *Int J Hydrogen Energy* 2017;42(32):20791–808.
- [27] Bae Suk Joo, Kim Seong-Joon, Lee Jin-Hwa, Song Inseob, Kim Nam-In, Seo Yongho, et al. Degradation pattern prediction of a polymer electrolyte membrane fuel cell stack with series reliability structure via durability data of single cells. *Appl Energy* 2014;131:48–55.
- [28] Morando S, Jemei S, Hissel D, Gouriveau R, Zerhouni N. ANOVA method applied to proton exchange membrane fuel cell ageing forecasting using an echo state network. *Math Comput Simul* 2017;1(131):283–94.
- [29] Morando S, Jemei S, Hissel D, Gouriveau R, Zerhouni N. Proton exchange membrane fuel cell ageing forecasting algorithm based on Echo State Network. *Int J Hydrogen Energy* 2017;42(2):1472–80.
- [30] Wu Y, Yuan M, Dong S, Lin L, Liu Y. Remaining useful life estimation of engineered systems using vanilla LSTM neural networks. *Neurocomputing* 2018;31(275):167–79.
- [31] Liu H, Mi X, Li Y. Smart multi-step deep learning model for wind speed forecasting based on variational mode decomposition, singular spectrum analysis, LSTM network and ELM. *Energy Convers Manage* 2018;1(159):54–64.
- [32] Borup R, Meyers J, Pivovar B, Kim YS, Muikundan R, Garland, et al. Scientific aspects of polymer electrolyte fuel cell durability and degradation. *Chem Rev* 2007;107:3904.
- [33] Yu PT, Gu W, Makharria R, Wagner FT, Gasteiger HA. The impact of carbon stability on PEM fuel cell startup and shutdown voltage degradation. *J Electrochem Soc* 2006;3(1):797–809.
- [34] Gu W, Carter RN, Yu PT, Gasteiger HA. Start/stop and local H₂ starvation

- mechanisms of carbon corrosion: model vs. experiment. *J Electrochem Soc* 2007;111(1):963–73.
- [35] Bi W, Gray GE, Fullera TF. PEM fuel cell Pt/C dissolution and deposition in nafion electrolyte. *Electrochem Solid State Lett* 2007;10(5):B101–4.
- [36] Shah A, Ralph TR, Walsha FC. Modeling and simulation of the degradation of perfluorinated ion-exchange membranes in PEM fuel cells. *J Electrochem Soc* 2009;156(4):B465–84.
- [37] Yuan Xiao-Zi, Li Hui, Zhang Shengsheng, Martin Jonathan, Wang Haijiang. A review of polymer electrolyte membrane fuel cell durability test protocols. *J Power Sources* 2011;196:9107–16.
- [38] Ma Rui, Liu Chen, Breaz Elena, Brøis Pascal, Gao Fei. Numerical stiffness study of multi-physical solid oxide fuel cell model for real-time simulation applications. *Appl Energy* 2018;226:570–81.
- [39] Gers FA, Schraudolph NN, Schmidhuber J. Learning precise timing with LSTM recurrent networks. *J Mach Learn Res* 2002;3:115–43.
- [40] Werbos Paul J. Backpropagation through time: what it does and how to do it. *Proc IEEE* 1990;78(10):1550–60.